JEE Journal of Ecological Engineering

Journal of Ecological Engineering 2024, 25(1), 336–344
https://doi.org/10.12911/22998993/175497
ISSN 2299–8993, License CC-BY 4.0

Received: 2023.08.11
Accepted: 2023.11.19
Published: 2023.12.05

Estimation of Photovoltaic Module Performance with L-Shaped Aluminum Fins Using Weather Data

Mohammad Hamdan[1], Eman Abdelhafez[2*], Akram Musa[3], Salman Ajib[4]

[1] Applied Science Private University, Renewable Energy Technology Department, Amman 11937, Jordan
[2] Al-Zaytoonah University of Jordan, Department of Alternative Energy Technology, Amman 11733, Jordan
[3] Amman Arab University, Department of Renewable Energy Engineering, Amman 11953, Jordan
[4] Department of Renewable Energies and Decentralized Energy Supplying, Faculty of Environmental Engineering and Applied Informatics, University of Applied Sciences and Arts, Campusallee 12, 32657 Lemgo, Germany
* Corresponding author's e-mail: eman.abdelhafez@zuj.edu.jo

ABSTRACT

Photovoltaic (PV) power prediction is vital for efficient and effective solar energy utilization within the energy ecosystem. It enables grid stability, cost savings, and the seamless integration of solar power into the broader energy infrastructure. In this work, previously obtained data on the estimation of the power produced by a PV, which is cooled by L-shaped aluminum fins attached to the backside of the PV at different spacings, is used to predict the power produced by the PV. This is achieved by employing both neural network models and multiple linear regression (MLR) techniques to assess the correlation between power generated by PV with L-shaped aluminum fins and its input variables. Two distinct approaches were employed for this purpose. The first approach involved the conventional MLR model, while the second utilized a neural network, specifically the multilayer perceptron (MLP) model. The estimated outcomes were subsequently compared against the previously measured data. The MLP model showed a great ability to identify the relationship between input and output variables, it was noted. The statistical error study provided evidence of data mining's acceptable accuracy when using the MLP model. Conversely, the results indicated that the MLR technique exhibited the least ability to estimate the power generated by PV with L-shaped aluminum fins.

Keywords: L-shaped aluminum fins, PV, artificial neural network, multiple linear regression.

INTRODUCTION

The rapid growth in demand for renewable energy sources has led to the increasing deployment of photovoltaic (PV) systems worldwide. However, the power generation is not achieved in its entirety due to multiple sources of losses. The most frequently encountered type of power loss results from the heat generated beneath the solar panel, which has a detrimental impact on the overall performance of the solar panel. The electrical energy produced is inversely related to the temperature of the base panel.

Enhancing the performance and efficiency of PV modules using different cooling methods, has become a paramount objective for researchers and industry professionals alike. There are several cooling methods used for PV cooling such as heat pipe technology [Alizadeh et al., 2018; Kianifard et al., 2020], phase change material [Nada and El-Nagar, 2018; Rajvikram et al., 2019; Sharma et al., 2009; Stropnik and Stritih, 2016; Shastry and Arunachala, 2020], microchannel heat transfer [Hamdan et al., 2018; Wang et al., 2019; Valeh-e-Sheyda et al., 2013; Rahimi et al., 2013], thermoelectric cooling [Ali et al., 2015; Benghanem et al., 2016; Najafi and Woodbury, 2013], nanotechnology [Verma et al., 2021; Behura and Gupta, 2020; Al-Sallal and Hamdan, 2022], optical methods [Al Aboushi et al., 2022; Hamdan and

Brawiesh, 2019], heat sink/fins/extended surfaces [Manasrah et al., 2020; Hamdan and Abdelhafez, 2021; Abdelhafez and Fava, 2022;].

The rapid growth in demand for renewable energy sources has led to the increasing deployment of photovoltaic systems worldwide. Enhancing the performance and efficiency of PV modules has become a paramount objective for researchers and industry professionals alike. One promising technique to augment the output of PV modules involves PV cooling using extended surfaces (fins), which are used as passive cooling devices. These fins effectively dissipate excess heat and, consequently, enhance the overall efficiency of the photovoltaic system [Abdelhafez and Fava, 2022; Hamdan et al., 2023; Behura et al., 2016; Prasad et al., 2014; Grubišić-Čabo et al., 2018; Akyol et al., 2021; Shiravi et al., 2022; Farhan and Hasan, 2020; Khan et al., 2020; Firoozzadeh et al., 2022].

Despite the advantages and solutions that photovoltaic generation offers, it faces considerable uncertainty and intermittency, primarily due to climatic factors like cloud cover, temperature fluctuations, and aerosols. Furthermore, a high penetration of PV systems in the distribution network adversely impacts the voltage levels at bus points. Collectively, these factors result in an impact on the grid for grid-connected PV power generation. Hence, achieving real-time and minimally delayed forecasting of the output power of PV is essential for efficiently managing power grid dispatching and regulation. It is also crucial for ensuring the seamless operation of PV power stations to optimize planning and distribution network functionality. Substantial research efforts have been devoted to forecasting power generated by PV systems.

Fan et al. [2014] proposed a data mining-based ensemble approach to predict next-day energy consumption and peak power demand. Outlier detection, recursive feature elimination, and genetic algorithm optimization were employed to enhance prediction accuracy. The ensemble models achieved MAPEs of 2.32% and 2.85% for next-day energy consumption and peak power demand, outperforming individual base models and enabling valuable applications in fault detection, operation optimization, and smart grid interactions.

An innovative technique for long-term solar forecasting was published by Alanazi et al. [2016], which used the Global Horizontal Irradiance (GHI) values and the neural networks toolbox as important factors. To improve forecast accuracy, their method merged pre- and post-processing processes. Meanwhile, Nomiyama et al. [2011] offered three separate methods using factor analysis, binary trees, and descriptive statistics to anticipate global solar radiation (GSR). These techniques used weather forecast data and the clearness index, derived as the ratio of GSR to extraterrestrial solar radiation, to forecast GSR at different lead times, including two days in advance, one day in advance, and three hours in advance.

Shi et al.'s [2012] prediction methods, which incorporate weather categorization and Support Vector Machines (SVM), are used to estimate the power production of solar systems. Four weather conditions were used to group the data: clear sky, overcast day, foggy day, and rainy day. They created a model for one-day forecasting of PV power output for a single station using historical power output data, weather forecast data, and SVMs.

To anticipate forthcoming solar insolation, Chung [2020] developed a multilayer feed-forward neural network model that takes into account current weather conditions. This model was utilized to predict the energy output of an actual PV system situated in South Korea. The accuracy of the model's energy production predictions was evaluated by comparing them to measured data. The results demonstrated promising accuracy metrics, with root mean squared error, mean bias error, and mean absolute error values. Nonetheless, further improvements are necessary to achieve dependable estimates for energy trading.

A solar radiation forecasting model using artificial neural networks (ANNs) and specialized methods was presented by Amrouche and Le Pivert [2014]. When the anticipated area lacked meteorological data, solar radiation was calculated using information from surrounding regions. The model offered daily forecasts for calculating PV system power generation. The daily PV energy production prediction model put forth by Long et al. [2014] was based on climatic variables. By categorizing meteorological data according to relevance and lowering the number of input variables, they increased the prediction algorithm's effectiveness.

Alhmoud et al.'s [2022] use of AI techniques allowed them to predict how much power the Jordanian Yarmouk University PV solar system would use up. The random forest model beat conventional prediction techniques, reaching a root mean squared error of 172.07 and a mean absolute error of 68.7, with an actual yield of 5548.96

MWh and a performance ratio (PR) of 95.73%. Through accurate forecasting, solar energy may be used to its fullest potential while reducing reliance on the grid. The study also provides useful information for operators to identify patterns in the historical data from Yarmouk University, enabling precise estimation of solar power usage. The control system and grid operators can now anticipate how much solar electricity will be used throughout the day.

Selimefendigil et al. [2018] conducted an experimental analysis and made performance predictions for solar photovoltaic modules equipped with porous fins using a dynamic artificial neural network-based multi-input multi-output system. Their study revealed that the addition of porous fins to the PV modules led to improved performance. The developed dynamic neural network-based mathematical model has the potential for further advancements and performance forecasts in such systems.

In the research by Sedaghat et al. [2019], they analytically calculated the annual energy output of a 50 W panel in both unfinned and pin-finned configurations. Their findings indicated that the power output increased by 1.24% to 4.16% when compared to the unfinned configuration, translating to an additional 1.04 kWh to 3.50 kWh of electrical energy production annually.

In the present work, ANN was used to predict the finned-cooled PV produced power. The L-shaped aluminum fins are attached to the backsides of four PVs, and the fins are arranged in an aligned manner and at a certain spacing. Previously obtained experimental data on the cooled PV were used in this work for training and validation of the used models. Such work and to the best of the authors such geometry at different spacing was conducted previously.

METHODOLOGY

Five PV panels arranged side by side for concurrent testing. The first module remained unaltered and served as the reference unit for comparison, while the other four panels were passively cooled using L-shaped aluminum fins functioning as heat sinks. These fins were positioned with different spacings on the backside of the modules: 2 cm for the second PV module, 4 cm for the third module, 6 cm for the fourth module, and 8 cm for the fifth module. Figure 1 illustrates the setup with all modules installed together for simultaneous measurements.

A GL220 data recorder was used to capture hourly temperature values for later examination. Each PV panel's power output was simultaneously measured and noted. A GRWS100 weather station also gathered information on the outside temperature, wind speed, humidity, and sun radiation. Daily from 9:00 a.m. to 4:00 p.m., the experimental work was conducted, with hourly data gathering. This involved taking readings of the surrounding air's temperature, wind speed, humidity, solar incident radiation, and each PV panel's output of power. The primary objective of this study is to forecast future PV power generation by employing an artificial neural network (ANN) based on the data obtained from previous observations.

In this study, a dataset comprising 155 samples were employed as independent variables for both the multilayer perceptron network and multiple

Figure 1. Experimental setup [Abdelhafez and Fava, 2022]

linear regression models. Additionally, the spacings between the fins, the average daily ambient temperature, average daily relative humidity, average daily wind speed, and average daily solar radiation were considered independent variables for both the MLP and multiple linear regression approaches. The output variable in this analysis was the average daily generated PV power.

RESULTS AND DISCUSSIONS

Multiple linear regression (classical method)

Multiple linear regression is a widely used statistical technique in data analysis and predictive modeling. It extends the concept of simple linear regression to accommodate multiple independent variables, enabling the exploration of complex relationships between the dependent variable and two or more predictors. In this method, the goal is to establish a linear equation that best fits the data, allowing for the estimation and prediction of the dependent variable based on the given set of independent variables. By assessing the strength and significance of each predictor's contribution, multiple linear regression offers valuable insights into the relative importance of various factors influencing the outcome. This versatile approach finds applications in numerous fields, including economics, social sciences, environmental studies, and engineering, where understanding and forecasting relationships between multiple variables are of paramount importance.

The multiple regression analysis incorporated input variables, including the spacings between the fins, average daily ambient temperature, average daily relative humidity, average daily wind speed, and average daily solar radiation. Meanwhile, the output variable was the power generated by PV with L-shaped aluminum fins. A total of 155 samples were utilized to derive the following linear equation.

$$Power = 0.014 \cdot wind\ speed - 0.034 \cdot relative\ humidity - 0.045 \cdot ambient\ temperature + 0.195 \cdot solar\ radiation - 0.034 \cdot distance + 5.844 \quad (1)$$

Table 1 offers an overview of the model, and Table 2 presents the equation's coefficients. It's important to highlight that the values of both R (coefficient of determination) and R^2 are notably influenced by the dependent variable, and this influence remains consistent across the spacings between the fins, average daily ambient temperature, average daily relative humidity, average daily wind speed, and average daily solar radiation.

As shown in Table 1, the correlation coefficient, denoted as R, provides insight into the strength and direction of the linear relationship between the predictor variables and the predicted variable. In this case, the reported R value is .985, suggesting a highly positive and strong correlation between the covariates (such as wind speed, humidity, temperature, radiation, and distance) and the power produced. The 'a' likely indicates a significant level, suggesting that the correlation is statistically significant. The R Square value, expressed as .971, represents the proportion of the variance in the dependent variable (power produced) that can be explained by the independent variables (covariates). A value of .971 indicates that approximately 97.1% of the variability in power production is accounted for by the model. This high R Square value signifies the model's effectiveness in capturing and explaining the patterns in the data. The adjusted R Square adjusts the R Square value to account for the number of predictors in the model. With an adjusted R Square of .970, the model not only demonstrates a high explanatory power but also avoids overfitting by penalizing the inclusion of unnecessary variables. This adjusted metric is particularly valuable when assessing the model's generalization to new, unseen data. The standard error of the estimate, reported as 2.0615, quantifies the average deviation of the observed values from the predicted values. A lower standard error indicates a more precise and accurate model. In this context, the relatively low standard error suggests that the model's predictions are, on average, close to the actual power production values.

Table 2 illustrates the correlation between various predictor variables, including the spacings between the fins, average daily ambient temperature, average daily relative humidity, average daily wind speed, and average daily solar radiation, all of which serve as inputs. These variables are analyzed in relation to the generated power, which is the dependent variable. In addition, it presents information on unstandardized coefficients, offering insights into the magnitude and direction of the impact that each covariate exerts on the predicted variable, namely power production. Examining the coefficients for individual covariates reveals the following: the constant has a coefficient of 5.844 and a t-value of

Table 1. Summary of the model

Model	R	R Square	Adjusted R Square	Std. error of the estimate
1	.985[a]	.971	.970	2.061500905438732

a – predictors: (constant), distance (cm), radiation1_Global rad. [W/m²], humidity 1m [%], WS_10 m [m/s], temp_1 m [°C].

Table 2. The coefficients of the model

Model		Unstandardized coefficients B	t
1	Constant	5.844	1.681
	Wind speed [m/s]	.014	0.073
	Humidity [%]	-.034	-1.299
	Temp [°C]	-.045	-.358
	Sloar radiation [W/m²]	.195	62.610
	Distance (cm)	-.034	-7.719

a – dependent variable: power produced (W).

1.681, representing the intercept of the regression equation and indicating an approximate power production of 5.844 when all covariates are zero. Wind speed, with a coefficient of 0.014 and a t-value of 0.073, demonstrates a positive association with a slight increase in power production, though this relationship may not be statistically significant due to the low t-value. Humidity [%] exhibits a negative coefficient of -0.034 and a t-value of -1.299, suggesting that higher humidity at 1 meter is associated with a decrease in power production, and this relationship appears to be statistically significant. Temperature [°C], on the other hand, has a negative coefficient of -0.045 and a low t-value of -0.358, indicating a potential decrease in power production with higher temperatures, but the relationship may not be statistically significant. Solar radiation [W/m²] displays a highly significant and positive relationship with a coefficient of 0.195 and a remarkably high t-value of 62.610, signifying a substantial increase in power production with an increase in global radiation. Finally, distance (cm) exhibits a significant negative relationship with a coefficient of -0.034 and a high t-value of -7.719, indicating a considerable decrease in power production as distance increases.

Multilayer perceptron model

The multilayer perceptron model is a prominent and powerful artificial neural network architecture widely used in various applications, including pattern recognition, classification, and regression tasks. It is a feedforward neural network that consists of multiple layers of interconnected neurons, with each layer containing an input layer, one or more hidden layers, and an output layer. The neurons in each layer are interconnected by weighted connections, and the model employs an activation function to introduce nonlinearity and enable complex learning patterns. MLPs are known for their ability to capture and model complex relationships within data, making them well-suited for handling intricate and high-dimensional datasets. Through a process known as backpropagation, the MLP model optimizes its weights during training to minimize the prediction error, making it a powerful tool for solving a wide range of problems, including image recognition, natural language processing, and financial forecasting.

This study employed the multilayer perceptron model to estimate the average daily power generated by PV with L-shaped aluminum fins. The MLP model was trained using five input variables, including the spacings between the fins, average daily ambient temperature, average daily relative humidity, average daily wind speed, and average daily solar radiation. The power generated by the PV system served as the output variable. The obtained results were compared and validated against the multiple regression technique.

The construction and testing of the MLP model were conducted using IBM SPSS Statistics 26 software. The dataset is divided into two main subsets: the training set and the testing set. The training set comprises 67.1% of the total sample, encompassing 104 cases, while the testing set represents 32.9%, consisting of 51 cases. This division is a standard practice in machine learning to assess how well a model generalizes to new, unseen data. The training set is utilized to train the model, enabling it to learn patterns and relationships within the data, while the testing set evaluates the model's performance on data it has not encountered during training. The valid category encompasses the entire dataset, indicating that all 155 cases are accounted for in the analysis. Importantly, no cases were excluded during the processing, suggesting that the entire dataset contributes to the development and evaluation of the predictive model as shown in table 3. Furthermore, the neural network includes one hidden layer with three units as shown in the table 4. The number of hidden layers and units is a crucial aspect of network design, influencing the model's capacity to capture intricate patterns in the data. The hyperbolic tangent activation function is chosen for the hidden layer, introducing non-linearity to the model and enabling it to learn complex relationships in the data. The output layer is responsible for producing the final prediction. In this case, the dependent variable is the power produced (W). The output layer consists of one unit, and the activation function is set to identity. The identity activation function is appropriate for regression problems, as it allows the network to directly output the predicted power values without introducing additional non-linear transformations. Similar to the input layer, the output layer's dependent variable is standardized. Standardizing the output ensures that the predictions are on a consistent scale, making it easier to interpret the model's performance and facilitating comparisons with other models. The error function, or loss function, is a critical component of the training process. The sum of squares is employed as the error function, reflecting the squared differences between predicted and actual values. Minimizing this error function during training guides the network towards making accurate predictions.

As shown in Table 5, the sum of squares error (SSE) is a fundamental metric that quantifies the squared differences between the predicted and actual values during the training phase. In this case, the SSE is reported as 1.904, providing insight into the overall training performance. The relative error, calculated as 0.037, represents the proportion of the error relative to the total variance in the data. These metrics collectively convey the model's ability to minimize discrepancies between predicted and actual power production values. During the training process, a stopping rule is employed to prevent overfitting and guide the model towards convergence. In this scenario, the stopping rule used involves monitoring the sum of squares error over consecutive steps. The training is halted if no decrease in error is observed for one consecutive step. This precautionary measure helps ensure that the model generalizes well to unseen data and does not overly adapt to noise in the training set. The model's performance is further evaluated on a separate testing dataset to assess its ability to generalize to new, unseen data. The sum of squares error for the testing phase is reported as 0.786, and the relative error

Table 3. Summary of the case processing

		N	Percent
Sample	Training	104	67.1%
	Testing	51	32.9%
Valid		155	100.0%
Excluded		0	
Total		155	

Table 5. MLP model summary

Training	Sum of squares error	1.904
	Relative error	.037
	Stopping rule used	1 consecutive step(s) with no decrease in error[a]
	Training time	0:00:00.00
Testing	Sum of squares error	.786
	Relative error	.041

Dependent variable: power produced (W)
a – error computations are based on the testing sample.

Table 4. MLP model information

Input layer	Covariates	1	WS_10 m [m/s]
		2	Humidity 1 m [%]
		3	Temp_1 m [°C]
		4	Radiation1_Global rad. [W/m²]
		5	Distance [cm]
	Number of units[a]		5
	Rescaling method for covariates		Standardized
Hidden layer(s)	Number of hidden layers		1
	Number of units in hidden layer 1[a]		3
	Activation function		Hyperbolic tangent
Output layer	Dependent variables	1	Power produced [W]
	Number of units		1
	Rescaling method for scale dependents		Standardized
	Activation function		Identity
	Error function		Sum of squares

a – excluding the bias unit.

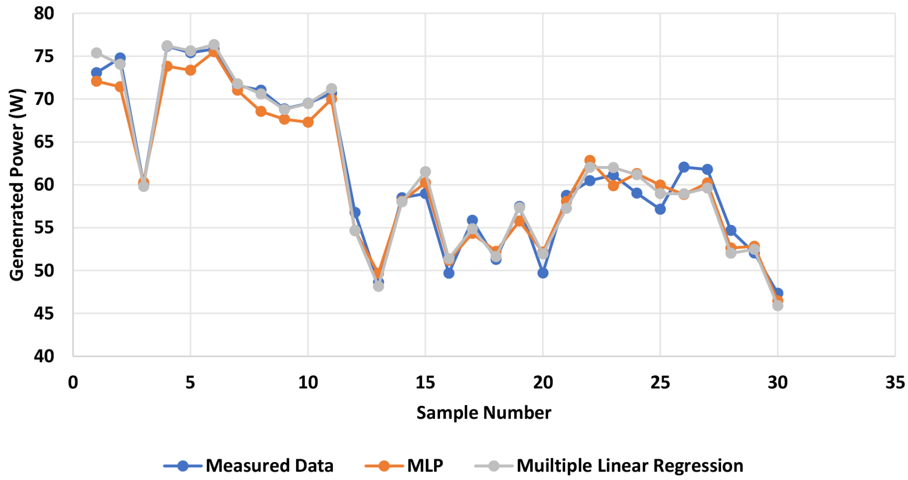

Figure 2. Contrast between the power output generated through experimentation and the power output predicted

is calculated as 0.041. These metrics offer an indication of the model's predictive accuracy and its ability to maintain consistent performance on data it has not encountered during training.

Figure 2 illustrates a contrast between the actual experimental data and the power estimates. Table 6 provides a summary of the performance comparison of the employed models through statistical analysis. Enhanced model accuracy is reflected by lower mean bias error (MBE) values, while increased accuracy is indicated by higher values of correlation coefficient (R) and root mean square error (RMSE).

It is to be noted that, generalizing photovoltaic findings from one location to another presents challenges due to diverse factors influencing solar installation performance. Although certain principles apply universally, the impact of site-specific variables must be carefully evaluated. Variables include climate and weather conditions, affecting solar irradiance and temperature sensitivity of PV panels. Geographical factors like latitude, altitude, and shading, along with environmental aspects such as pollution, impact system efficiency. Grid infrastructure variations and regulatory disparities, including incentives and permitting, also play pivotal roles. Additionally, installation quality, technology changes, and evolving PV technologies contribute to performance discrepancies. To accurately predict PV system performance, it is imperative to conduct a site-specific analysis, utilizing tools like solar resource assessment software and considering local conditions. A feasibility study or pilot project in the new location is recommended for a precise evaluation of performance under distinct local circumstances. Furthermore, using artificial neural networks for predicting photovoltaic power production comes with challenges and limitations that must be addressed for reliable results. Issues include the need for large and diverse datasets, the risk of overfitting and model complexity, the importance of relevant feature selection, difficulties in capturing temporal and spatial variations, and the "black box" nature of ANNs, making interpretation challenging. Computational intensity, generalization to extreme conditions, and limitations in robustness and physical understanding are also notable concerns. Overcoming these limitations involves meticulous data preprocessing, thoughtful model design, rigorous validation, and ongoing model maintenance.

Looking into the future of research in PV power prediction using ANNs, several potential directions emerge. Hybrid models combining ANNs with other machine-learning techniques or physical models may be explored for improved accuracy and robustness. Enhancing the interpretability of ANN models through explainable AI (XAI), applying transfer learning to address spatial

Table 6. Comparison of performance of the employed models through statistical analysis

Model	R	RMSE	MBE
Multiple linear regression	0.985	2.025	0.155
Multilayer perceptron network	0.982	2.308	0.118

variability, developing online learning algorithms for continuous adaptation, and incorporating uncertainty quantification methods are avenues for further exploration. Advanced feature engineering, data augmentation techniques, edge computing for real-time predictions, integration with physical models, and extending ANN models for fault detection and diagnostics are areas of interest. Additionally, establishing benchmark datasets and standard evaluation metrics, along with real-time adaptation techniques, will contribute to the ongoing improvement of ANN-based models for PV power prediction in the renewable energy industry.

CONCLUSIONS

In this study, multiple linear regression technique and neural network models were employed to establish the connection between the power generated by photovoltaics systems with L-shaped aluminum Fins and its input variables. Two different approaches were utilized to achieve this goal. The first method followed a traditional path employing a model, while the second approach harnessed the multilayer perceptron network.

Comparisons between the predicted data and the actual experimental data revealed that the multilayer perceptron network model successfully captured the connection between input and output variables. Additionally, the statistical error analysis affirmed the precision of utilizing the MLP model for this estimation. In contrast, the results indicated that the multiple linear regression model exhibited the least capability in accurately estimating the power generated by PV systems with L-shaped aluminum fins.

REFERENCES

1. Abdelhafez E., Fava S. 2022. Performance of a PV module using water based titanium oxide nano fluid coated fins. International Journal on Energy Conversion (IRECON), 10(2), 52-59.
2. Akyol U., Akal D., Durak A. 2021. Estimation of power output and thermodynamic analysis of standard and finned photovoltaic panels. Energy Sources, Part A: Recovery, Utilization, and Environmental Effects, 45(3), 8438–8457.
3. Al Aboushi A., Abdelhafez E., Hamdan M. 2022. Finned PV natural cooling using water-based TiO2 nanofluid. Sustainability, 14(20), 12987.
4. Alanazi M., Alanazi A., Khodaei A. 2016. Long-term solar generation forecasting. 2016 IEEE/PES Transmission and Distribution Conference and Exposition (T&D), Dallas, TX, USA.
5. Alhmoud L., Al-Zoubi A. M., Aljarah I. 2022. Solar PV power forecasting at Yarmouk University using Machine Learning Techniques. Open Engineering, 12(1), 1078–1088.
6. Ali M., Ali H., Moazzam W., Saeed M.B. 2015. Performance enhancement of PV cells through micro-channel cooling. AIMS Energy, 3(4), 699–710.
7. Alizadeh H., Ghasempour R., Shafii M.B., Ahmadi M.H., Yan W., Nazari M.A. .2018. Numerical simulation of PV cooling by using single turn pulsating heat pipe. International Journal of Heat and Mass Transfer, 127, 203–208.
8. Al-Sallal H., Hamdan M. 2022. Bifacial photovoltaic (PV) systems performance enhancement using a selective surface reflector. International Journal on Energy Conversion (IRECON), 10(2), 37.
9. Amrouche B., Le Pivert X. 2014. Artificial Neural Network based daily local forecasting for Global Solar Radiation. Applied Energy, 130, 333–341.
10. Behura A.K., Gupta H. K. 2020. Efficient direct absorption solar collector using nanomaterial suspended heat transfer fluid. Materials Today: Proceedings, 22, 1664–1668.
11. Behura A.K., Prasad B.N., Prasad L. 2016. Heat transfer, friction factor and thermal performance of three sides artificially roughened Solar Air Heaters. Solar Energy, 130, 46–59.
12. Benghanem M., Al-Mashraqi A.A., Daffallah K.O. 2016. Performance of solar cells using thermoelectric module in hot sites. Renewable Energy, 89, 51–59.
13. Chung M.H. 2020. Estimating solar insolation and power generation of photovoltaic systems using previous day weather data. Advances in Civil Engineering, 2020, 1–13.
14. Fan C., Xiao F., Wang S. 2014. Development of prediction models for next-day building energy consumption and peak power demand using data mining techniques. Applied Energy, 127, 1–10.
15. Farhan A.A., Hasan D.J. 2020. An experimental investigation to augment the efficiency of photovoltaic panels by using longitudinal fins. Heat Transfer, 50(2), 1748–1757.
16. Firoozzadeh M., Shiravi A.H., Chandel S.S. 2022a. An experimental analysis of enhancing efficiency of photovoltaic modules using straight and Zigzag Fins. Journal of Thermal Analysis and Calorimetry, 147(16), 8827–8839.
17. Grubišić-Čabo F., Nižetić S., Čoko D., Marinić Kragić I., Papadopoulos A. 2018. Experimental investigation of the passive cooled free-standing

photovoltaic panel with fixed aluminum fins on the backside surface. Journal of Cleaner Production, 176, 119–129.

18. Hamdan M., Abdelhafez E. 2021. The impact of optical liquid filters on PV panel performance. Environmental Science and Pollution Research, 29(16), 23988–23993.
19. Hamdan M., Abdelhafez E., Al Aboushi A., Othman A., Al-Saleh S., Ajib S. 2023. Enhancing PV modules performance using L-shaped aluminum fins. International Review of Mechanical Engineering (IREME), 17(2), 48-56.
20. Hamdan M., Brawiesh A.K. 2019. Enhancement of PV performance using optical solar spectrum splitting. Energy Sources, Part A: Recovery, Utilization, and Environmental Effects, 43(16), 2000–2007.
21. Hamdan M., Shehadeh M., Al Aboushi A., Hamdan A., Abdelhafez, E. 2018. Photovoltaic cooling using phase change material. Jordan Journal of Mechanical and Industrial Engineering, 12(3), 167-170.
22. Khan S., Waqas A., Ahmad N., Mahmood M., Shahzad N., Sajid M. B. 2020. Thermal management of solar PV module by using hollow rectangular aluminum fins. Journal of Renewable and Sustainable Energy, 12(6).
23. Kianifard S., Zamen M., Nejad A.A. 2020. Modeling, designing and fabrication of a novel PV/T cooling system using half pipe. Journal of Cleaner Production, 253, 119972.
24. Long H., Zhang Z., Su Y. 2014. Analysis of daily solar power prediction with data-driven approaches. Applied Energy, 126, 29–37.
25. Manasrah A., Alkhalil S., Masoud M. 2020. Investigation of multi-way forced convective cooling on the backside of solar panels. International Journal on Energy Conversion (IRECON), 8(5), 181.
26. Nada S., El-Nagar D. 2018. Possibility of using PCMs in temperature control and performance enhancements of free stand and building integrated PV modules. Renewable Energy, 127, 630–641.
27. Najafi H., Woodbury K. 2013. Optimization of a cooling system based on peltier effect for photovoltaic cells. Solar Energy, 91, 152–160.
28. Nomiyama F., Asai J., Murakami T., Murata J. 2011. A study on global solar radiation forecasting using weather forecast data. IEEE 54th International Midwest Symposium on Circuits and Systems.
29. Prasad B.N. Behura A.K., Prasad L. 2014. Fluid flow and heat transfer analysis for heat transfer enhancement in three sided artificially roughened Solar Air Heater. Solar Energy, 105, 27–35.
30. Rahimi M., Karimi E., Asadi M., Valeh-e-Sheyda P 2013. Heat transfer augmentation in a hybrid microchannel solar cell. International Communications in Heat and Mass Transfer, 43, 131–137.
31. Rajvikram M., Leoponraj S., Ramkumar S.P., Akshaya H., Dheeraj A. 2019. Experimental investigation on the abasement of operating temperature in solar photovoltaic panel using PCM and aluminium. Solar Energy, 188, 327–338.
32. Sedaghat A., Karami M.R. Eslami M. 2019. Improving performance of a photovoltaic panel by Pin Fins: A theoretical analysis. Iranian Journal of Science and Technology, Transactions of Mechanical Engineering, 44(4), 997–1004.
33. Selimefendigil F., Bayrak F., Oztop H.F. 2018. Experimental Analysis and dynamic modeling of a photovoltaic module with porous fins. Renewable Energy, 125, 193–205.
34. Sharma A., Tyagi V., Chen C., Buddhi D. 2009. Review on thermal energy storage with phase change materials and applications. Renewable & Sustainable Energy Reviews, 13(2), 318–345. https://doi.org/10.1016/j.rser.2007.10.005
35. Shastry D.M.C., Arunachala U.C. 2020. Thermal management of photovoltaic module with Metal Matrix Embedded PCM. Journal of Energy Storage, 28, 101312.
36. Shi J., Lee W.-J., Liu Y., Yang Y., Wang P. 2012. Forecasting power output of photovoltaic systems based on weather classification and support Vector Machines. IEEE Transactions on Industry Applications, 48(3), 1064–1069.
37. Shiravi A.H., Firoozzadeh M. 2022. Performance assessment of a finned photovoltaic module exposed to an air stream: An experimental study. Journal of the Brazilian Society of Mechanical Sciences and Engineering, 44(11).
38. Stropnik R., Stritih U. 2016. Increasing the efficiency of PV panel with the use of PCM. Renewable Energy, 97, 671–679.
39. Valeh-e-Sheyda P., Rahimi M., Karimi E., Asadi M. 2013. Application of two-phase flow for cooling of hybrid microchannel PV cells: A comparative study. Energy Conversion and Management, 69, 122–130.
40. Verma S. Mohapatra S., Chowdhury S., Dwivedi G. 2021. Cooling techniques of the PV module: A Review. Materials Today: Proceedings, 38, 253–258.
41. Wang R., Wang J., Yuan W. 2019. Analysis and optimization of a microchannel heat sink with V-ribs using nanofluids for micro solar cells. Micromachines, 10(9), 620.